N76-28178

COMPARISON OF VORTEX LATTICE PREDICTED FORCES WITH WIND TUNNEL EXPERIMENTS FOR THE F-4E(CCV) AIRPLANE WITH A CLOSELY COUPLED CANARD

Lloyd W. Gross

McDonnell Aircraft Company

SUMMARY

The McDonnell Douglas F-4E (CCV) wind tunnel model with closely coupled canard control surfaces was analyzed by means of a version of a Vortex Lattice program that included the effects of nonlinear leading edge or side edge vortex lift on as many as four individual planforms. The results were compared with experimental data from wind tunnel tests of a 5-percent scale model tested at a Mach number M = 0.6. The comparison was facilitated by drawing the respective lift or thrust force vectors on the lift vs drag polar diagram. It indicated that nonlinear vortex lift developed on the side edges due to tip vortices, but did not appear to develop on the leading edges within the range of angles of attack that were studied. Instead, substantial leading edge thrust was developed on the lifting surfaces.

A configuration buildup illustrated the mutual interference between the wing and control surfaces. The effect of adding a lifting surface behind existing surfaces is to increase the loading on the forward surfaces. Similarly, adding a forward surface decreases the load on the following surfaces. On the configuration studied, addition of the wing increased the loading on the canard, but the additional load on the canard due to adding the stabilator was small. The effect of the wing on the stabilator was to reduce the static stability contribution of the stabilator. Then, when the canard was added, the stabilator suffered an additional loss of static stability contribution, in contrast to the effect on the canard of adding the stabilator.

This study verified the usefulness of the Vortex Lattice program as a predictive tool. It pointed up the need for a version capable of including vertical panels so that side forces and yawing moments can be included. Also, the ability to add independent planforms outboard of existing planforms, with a proper carry-over of lift, would facilitate the study of "all-movable" control surfaces.

15

INTRODUCTION

The McDonnell Aircraft Company has been using the Vortex Lattice program developed by Margason and Lamar of the NASA Langley Research Center (Reference 1) for the design and analysis of aircraft configurations having

single or multiple planforms with good results (unpublished studies similar to those of Reference 2). However, the available program was an early version of limited capability. The advent of versions having enhanced capability increases the potential for the use of the method as long as rules can be established to define the applicable ranges of the pertinent parameters. The version that currently has been made available by NASA (LRC Program No. A4737) includes the prediction of nonlinear leading edge and side edge vortex lift detailed in Reference 3 and has provision for as many as four planforms which can be arranged asymmetrically. This version of the Vortex Lattice program was developed by James Luckring of the NASA Langley Research Center.

A method of airplane control that is receiving new emphasis is the use of canards or control surfaces forward of the main lifting surface. This form of control has been made attractive by advances in active control technology that allow reduced or negative static stability. Also, it has been determined that the interference between the wing and canard is such that direct lift control and direct side force control can be achieved (Reference 4). These ideas have been explored by many agencies, among which are a series of wind tunnel tests conducted as part of the USAF Flight Dynamics Laboratory Fighter Control Configured Vehicle (CCV) programs. Various horizontal and vertical canard planforms were tested on several models of the McDonnell Douglas YF-4E airplane (e.g., Reference 5). The close-coupled, fully operable horizontal canards then were test-flown on an YF-4E under the MCAIR-sponsored Precision Aircraft Control Technology (PACT) program. These tests verified the use of canards for maneuverability enhancement and additional degrees of freedom of the flight path.

The use of canards on the YF-4E (PACT) airplane generated an interest in predicting all of their effects. The Vortex Lattice program has been shown to be useful in the prediction of the wing-canard interference (Reference 2), but it had been limited by the restriction to two planforms. Once the four-planform version of the program became available, a more complex configuration could be studied. In particular, it was of interest to determine how well the Vortex Lattice program predicted the multiple lifting surface interactions and to what extent the various elements generated nonlinear vortex lift. Direct side force control could not be studied since there was no provision for vertical paneling. For a study of the longitudinal forces and moments, the wind tunnel model of Reference 5 was analyzed in order to provide a comparison with the experimental data. In addition to the analysis of the specific configurations for which experimental data was available, a complete configuration buildup was made to give an indication of the interference that existed between the components of the configuration.

SYMBOLS

b	wing span
c	wing or control surface chord

c_ℓ	wing or control surface section lift coefficient
C_D	total drag coefficient
C_{D_o}	total drag coefficient at zero degrees angle of attack
C_L	total lift coefficient
C_{L_o}	total lift coefficient at zero degrees angle of attack
C_M	total moment coefficient based on mean aerodynamic chord
C_N	total normal force coefficient
C_{N_p}	total normal force coefficient due to potential flow normal force on deflected control surface
C_{N_s}	total normal force coefficient due to nonlinear leading edge thrust of deflected control surface
C_{N_r}	total normal force coefficient due to nonlinear leading edge vortex lift of deflected control surface
C_S	total leading edge suction force coefficient
C_T	total leading edge thrust coefficient
C_{T_p}	total leading edge thrust coefficient due to potential flow normal force on deflected control surface
C_{T_s}	total leading edge thrust coefficient due to leading edge thrust of deflected control surface
C_{T_r}	total leading edge thrust coefficient due to nonlinear vortex lift of deflected control surface
C_v	total vortex force coefficient (Polhamus Effect)
C_Y	total side force coefficient rotated to normal force direction (Polhamus Effect)
K_c	constant
K_p	kernel of potential flow normal force (defined in reference 3)
K_{p_a}	kernel of potential flow normal force for undeflected portion of planform
K_{p_b}	kernel of potential flow normal force for deflected control surface

$K_{V,LE}$	kernel of nonlinear leading edge suction force (defined in reference 3)
$K_{V,SE}$	kernel of nonlinear side edge thrust (defined in reference 3)
K_{V,LE_b}, K_{V,SE_b}	kernels of nonlinear forces for deflected control surface
MAC	mean aerodynamic chord
y	distance from aircraft centerline in wingtip direction
α	angle of attack
δ	control surface deflection
δ_c	canard deflection
δ_r	control surface deflection including rotation for Polhamus Effect

MODEL CONFIGURATION

The YF-4E (PACT) is equipped with a 1.86 m^2 auxiliary control surface and related fairing located just aft of and above the engine inlet on each side (Figure 1). The canard is an active control surface with the associated actuators and electronics. The wing includes leading edge slats on both inboard and outboard panels. The wind tunnel model, against which the analysis was checked, is of 5-percent scale and also includes the leading edge slats. The model was tested over a range of Mach numbers from M = 0.6 to M = 1.98, although the analysis is resticted to a Mach number M = 0.6. The configurations that were tested include the basic airplane, the basic airplane without stabilator and the basic airplane with horizontal canard. The model was not tested with all of the configurations that normally would make up a full configuration buildup. In particular, the configuration with canard and wing but with the stabilator removed was not tested. Also, the design of this model precluded the removal of the wings.

The planform configurations used to represent the aircraft model are shown as Figure 2. The aft fuselage and stabilator configuration was changed from that of the model in order to keep the stabilator effective, but no attempt was made to determine whether this configuration change was necessary to match experiment. A list of the configurations that were analyzed is given as Table 1. The configurations for which experimental data are available also are noted.

RESULTS AND DISCUSSION

Control Surfaces Undeflected

The results of the analysis are compared with experiment in Figures 3 and 4. These figures show the usual presentation of the lift coefficient versus angle of attack and moment coefficient versus lift coefficient in Figures 3(a) through 3(c) for the three configurations for which experimental data are available. The lift coefficient versus drag coefficient polars are compared with experiment for these configurations in Figures 4(a) through 4(c). The three curves shown in each figure represent the end points of the force vectors identifiable by potential flow theory. The first curve is the sum of the lift and induced drag forces due to integration of the incremental vortex forces induced at right angles to the vortex lattice (potential flow normal forces). The second is the combination of the potential flow normal force and the nonlinear thrust force induced in the direction of the vortex lattice (leading edge suction or thrust). The third is the combination of the potential flow normal force and the nonlinear forces normal to the vortex lattice induced by the presence of vorticity in the flow field near a sharp leading or side edge (vortex force). The magnitudes of the vortex forces are found by rotating the leading edge suction force or side edge force through ninety degrees (Polhamus Effect, Reference 6).

Conclusions might be drawn from Figures 3 and 4 but it is difficult to determine what percentage of leading edge thrust or vortex lift has been achieved. This becomes more obvious if the forces are drawn in vectorial form as in Figures 5(a) through 5(c). In this case the scales are not distorted as they are in Figure 4 so that the angular relationships can be appreciated. Since the drag direction is coincident with the freestream direction, the potential flow normal force is inclined to the lift force direction by the angle of attack. This vector is not drawn in order to reduce the number of lines but it locates the origin of the subsequent vectors. The side force vector is directed normal to the plane of the paper but appears in the direction of the potential flow normal force when rotated by the presence of the tip vortex. The leading edge suction force and the component of this vector in the thrust direction are at right angles to the potential flow normal force. The Polhamus Effect is illustrated by rotating the leading edge suction force to lie in the direction of the normal force.

The three examples for which experimental comparisons are available have had their force vectors for the midrange of angles of attack combined as Figure 6. It can be seen that there is a good agreement between experiment and analysis when the leading edge thrust effect is considered. Thus, at these angles of attack, there does not seem to be any leading edge vortex lift.

In order to evaluate the pitching moment predictions of the vortex lattice method, the longitudinal static stability was determined from Figures 3(a) through 3(c) and compared with experiment in Table II. Since the longitudinal static stability contribution of the vortex lift is zero at a lift coefficient of zero, its contribution was evaluated at the intermediate lift coefficient $C_L = 0.3$.

The distance to the centroid of lift from the normal reference center, expressed in terms of the wing mean aerodynamic chord, also is given in Table II. And since the centroid as calculated includes a portion of the fuselage lift, the distance from the model balance center to the quarter-chord of the mean aerodynamic chord for each lifting surface is included. It can be seen that in all three cases the analytical static stability is more negative than are the experimental values. Since the case without the stabilator shows good agreement and the cases with the stabilator show poorer agreement, it would appear that the stabilator as modeled is too effective. However, it was felt that additional studies to determine how best to model the tail in order to more closely match experiment were beyond the scope of this investigation.

Effect of Control Surface Deflection

While vortex lift did not seem to form on the wing or control surfaces under standard flight conditions, it could form on thin control surfaces that had been deflected through an appreciable angle. But in order to isolate the effect of the deflected control surface, it was necessary to evaluate the force vectors in detail. To do this, a purely geometrical study was resorted to. The first assumption was that the leading edge sunction force vector of the control surface was in the direction of the twist angle of the leading edge panel. Thus, the single planform is made up of the untwisted part and the twisted part b (Figure 7) whose principle force directions are separated by the twist angle. It was further assumed that the total potential flow force as given by the program was determined by the integration of the force produced by the horseshoe vortices in the direction normal to the vortex lattice. In the same way, it was assumed that the total nonlinear force was determined by the integration of these vortex singularity forces in the direction of the vortex lattice. Then the forces of the individual panels can be written in terms of the given forces of the total planform (see Figure 7 for definition of the appropriate vectors).

Normal Forces:

$$K_p \sin\alpha \cos\alpha + C_{L_o} = K_{p_a} \sin\alpha \cos\alpha + K_{p_b} \sin(\alpha+\delta) \cos(\alpha+\delta) \cos\delta$$

Leading Edge Suction:

$$K_{V,LE} \sin^2\alpha + K_c = - K_{p_b} \sin(\alpha+\delta) \cos(\alpha+\delta) \sin\alpha + K_{V,LE_b} \sin^2(\alpha+\delta) \cos\delta$$

where δ is the twist angle of the control surface and K_p, $K_{V,LE}$, and C_{L_o} are known from the Vortex Lattice program solution.

At an angle of attack $\alpha = 0°$

$$C_{L_o} = K_{p_b} \sin\delta \cos^2\delta$$

$$K_c = - K_{p_b} \sin^2\delta \cos\delta + K_{V,LE_b} \sin^2\delta \cos\delta$$

These are two equations for the four unknowns K_c, K_{p_a}, K_{p_b}, and K_{V,LE_b}. To provide the other two equations, the solutions are matched at $\alpha = -\delta$ so that

$$-K_p \sin\delta \cos\delta + C_{L_o} = K_{p_a} \sin\delta \cos\delta$$

$$K_{V,LE} \sin^2\delta + K_c = 0$$

Then,

$$K_c = -K_{V,LE} \sin^2\delta \qquad K_{p_a} = -\frac{C_{L_o}}{\sin\delta \cos\delta} + K_p$$

$$K_{V,LE_b} = K_{p_b} - \frac{K_{V,LE}}{\cos\delta} \qquad K_{p_b} = \frac{C_{L_o}}{\sin\delta \cos^2\delta}$$

and $K_{V,SE_b} = K_{V,SE}$ since the integration of the side forces is unchanged by the fact that the control surface is rotated.

Resolving the forces on the control surface to the principal normal force and thrust force directions of the basic configuration:

Control Surface Potential Flow Force:

$$C_{N_p} = K_{p_b} \sin(\alpha+\delta) \cos(\alpha+\delta) \cos\delta$$

$$C_{T_p} = -K_{p_b} \sin(\alpha+\delta) \cos(\alpha+\delta) \sin\delta$$

Control Surface Leading Edge Suction Force:

$$C_{N_s} = K_{V,LE_b} \sin^2 (\alpha+\delta) \sin\delta$$

$$C_{T_s} = K_{V,LE_b} \sin^2 (\alpha+\delta) \cos\delta$$

Control Surface Suction Force with Polhamus Effect

$$C_{N_r} = (K_{V,LE_b} + K_{V,SE_b}) \sin^2 (\alpha+\delta) \sin\delta_r$$

$$C_{T_r} = (K_{V,LE_b} + K_{V,SE_b}) \sin^2 (\alpha+\delta) \cos\delta_r$$

where

$$\delta_r = \delta + \frac{\alpha+\delta}{|\alpha+\delta|} \frac{\pi}{2}$$ to give the proper direction of rotation.

The method of vectorial addition of the forces of the undeflected and deflected surfaces is illustrated in Figure 7. The lift vs drag polar for the complete configuration with the canard deflected 20° is shown in Figure 8. It can be seen that the vectorial representation gives a closer agreement with the experimental results than does the case where the force coefficient kernels K_p, $K_{V,LE}$ and $K_{V,SE}$ are all grouped together linearly. In this case, the agreement would appear to be enhanced if the side edge normal forces were

discounted as well.

Lifting Surface Effectiveness

One method of determining the interference between the components of a complete configuration would be an evaluation of the potential flow normal force coefficient kernels K_p. Another, more graphic, method is to look at the span loading for the individual components. In this case the span loadings are compared at a constant angle of attack $\alpha = 16.45°$. This angle of attack gives an overall lift coefficient $C_L = 1.0$ for the configuration including both canard and stabilator. Figure 9 shows the total span loading for the three cases with interfering flows. The integrated lift is approximately the same for all three cases; in fact, there is less than a 3% difference between the highest and the lowest total lift coefficient.

The span loadings on the individual components are given as Figures 10(a) through 10(c). The wing loadings are shown as Figure 10(a) and it can be seen that the presence of the canard decreases the total wing lift whereas the presence of the stabilator increases it. However, with the canard in place, the additional presence of the stabilator causes only a small increase of wing lift. The effect of the additional lifting surfaces on the canard is similar as can be seen in Figure 10(b). The total lift on the canard alone is increased by the presence of the wing and the additional presence of the stabilator causes only a very small additional lift.

However, the stabilator is much more sensitive to the presence of additional lifting elements as can be seen in Figure 10(c). As a surface acting alone, the stabilator can carry a good load. The presence of the wing substantially decreases the lift-curve slope so that the load carried at this angle of attack is much less than it would be if the stabilator were acting alone. The addition of the canard further decreases the static stability contribution of the stabilator. In this case the stabilator lift-curve slope is only one-tenth of the lift curve slope of the stabilator acting alone. This effect is analogous to the "cascading of lift" discussed in Reference 7 with respect to multi-element airfoils. In each case the addition of a lifting element causes the lift of forward elements to be increased and that of following elements to be decreased.

CONCLUSIONS

The Vortex Lattice program has been shown by comparison with wind tunnel tests to accurately calculate the normal forces of aircraft, even when multiple elements with strong interactions are present. This is true up to angles of attack where strong viscous-inviscid interactions become important. Calculation of the leading edge thrust also is good. These conclusions hold even for the case of deflected control surfaces as long as the force vectors are properly directed. Prediction of the longitudinal pitching moment was less satisfactory due to the stabilator paneling that was chosen.

The 5% scale model of the F-4E (CCV) aircraft apparently did not develop leading edge vortex lift up to the angles of attack where the viscous interactions predominate. Although the lifting surface leading edges are round, their thickness to chord ratios are small enough that leading edge boundary layer separation should occur. Unfortunately, the presence of the leading edge slat clouds the comparison so that general conclusions can not be drawn.

Two possible improvements have suggested themselves during this study. The first is the inclusion of vertical panels so that vertical control surfaces or fuselage surfaces can be modeled. This would allow the study of phenomena such as direct side-force control due to differentially deflected canards. The second is provision for the spanwise stacking of planforms (e.g., a canard and forward fuselage) with a proper carry-over of lift. In this way, the effect of deflected control surfaces could be studied without having to separate the contributions of the deflected and undeflected parts as was done in this study.

REFERENCES

1. Margason, R. J. and Lamar, J. E., "Vortex-Lattice Fortran Program for Estimating Subsonic Aerodynamic Characteristics of Complex Planforms," NASA TN D-6142, February 1971.

2. Gloss, B. B., "Effect of Canard Location and Size on Canard-Wing Interference and Aerodynamic Center Shift Related to Maneuvering Aircraft at Transonic Speeds," NASA TN D-7505, June 1974.

3. Lamar, J. E. and Gloss, B. B., "Subsonic Aerodynamic Characteristics of Interacting Lifting Surfaces with Separated Flow Around Sharp Edges Predicted by a Vortex-Lattice Method," NASA TN D-7921, September 1975.

4. Stumpfl, S. C. and Whitmoyer, R. A., "Horizontal Canards for Two-Axis CCV Fighter Control," Presented to AGARD Symposium on "Impact of Active Control Technology in Airplane Design," AGARD CPP-157, October 1974.

5. Voda, J. J., "Summary of Results of Series II and III High Speed Wind Tunnel Tests of a 5-percent Scale Model F-4E (CCV), AEDC 4-foot Transonic Wind Tunnel Test No. 242," McDonnell Douglas Report MDC A2129, December 1972.

6. Polhamus, E. C., "A Concept of the Vortex Lift of Sharp-Edged Delta Wings Based on a Leading-Edge-Suction Analogy," NASA TN D-3767, 1966.

7. Smith, A. M. O., "High-Lift Aerodynamics," 37th Wright Brothers Lecture, Journal of Aircraft, V. 12, No. 6, June 1975.

TABLE I

CONFIGURATIONS STUDIED

1. Fuselage Alone
2. Fuselage + Canard
*3. Fuselage + Wing
4. Fuselage + Stabilator
5. Fuselage + Wing + Canard
*6. Fuselage + Wing + Stabilator
*7. Fuselage + Wing + Canard + Stabilator

*Experimental Comparison Available.

TABLE II

LONGITUDINAL PITCHING MOMENT PREDICTION

	Static Stability, $(\frac{dC_M}{dC_L})$			Distance to Normal Force Centroid from Moment Center		
	Experimental	Predicted				
		Linear (C_L=0)	Vortex (C_L=0.3)	Canard	Wing	Stabilator
Fuselage + Wing	0.044	0.032	0.086		-0.0536	
Fuselage + Wing + Stabilator	0	-.133	-.143		0	-1.4046
Fuselage + Wing + Canard + Stabilator	.086	.054	.035	0.7836	-.1109	-1.6630
Distance to 1/4 MAC from Moment Center				.5790	.08	-1.4369

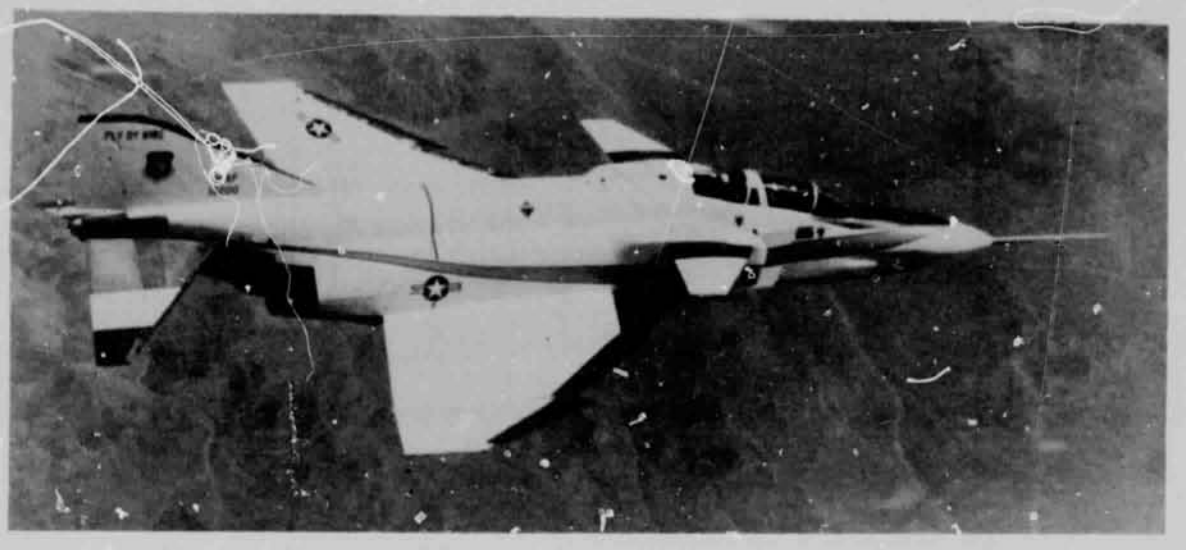

Figure 1.- McDonnell Douglas YF-4E (PACT) airplane.

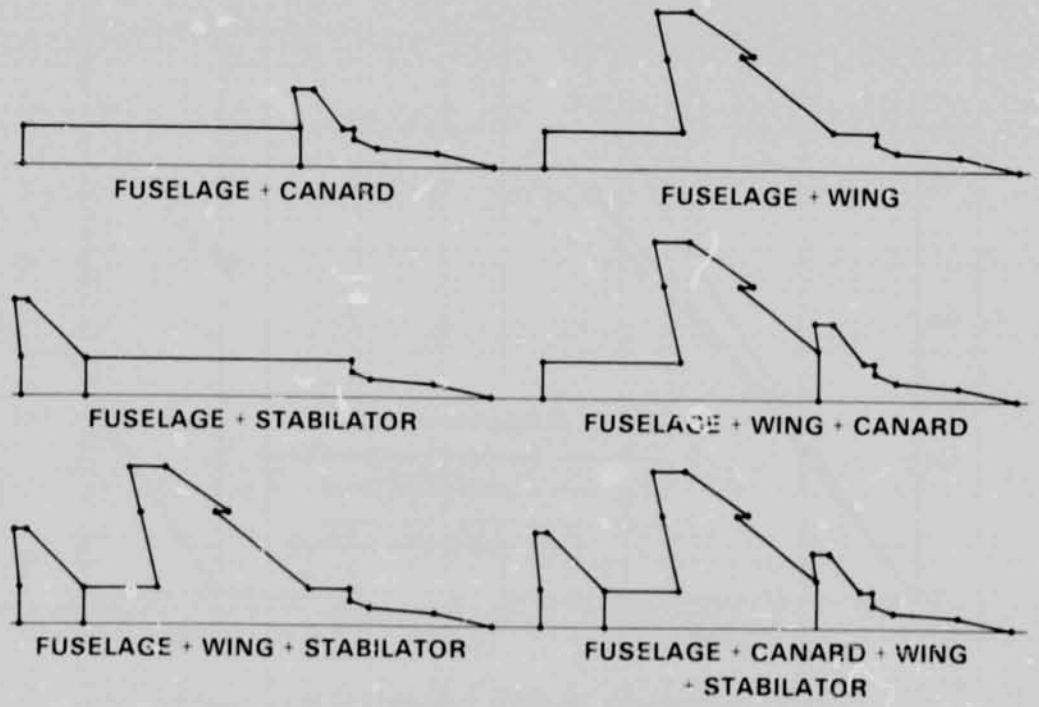

Figure 2.- Planform configurations of the McDonnell Douglas F-4E (CCV) studied.

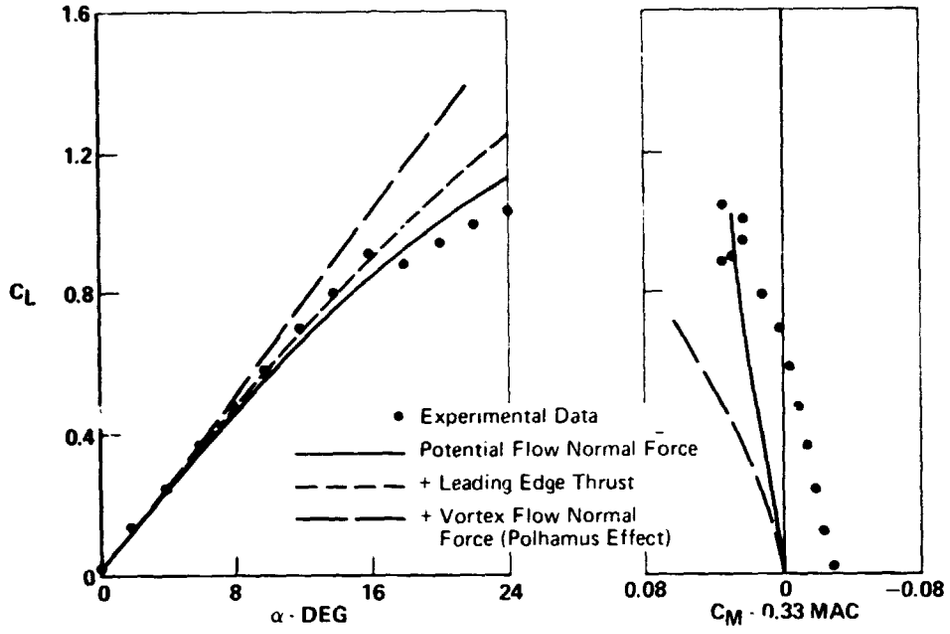

(a) Fuselage + wing.

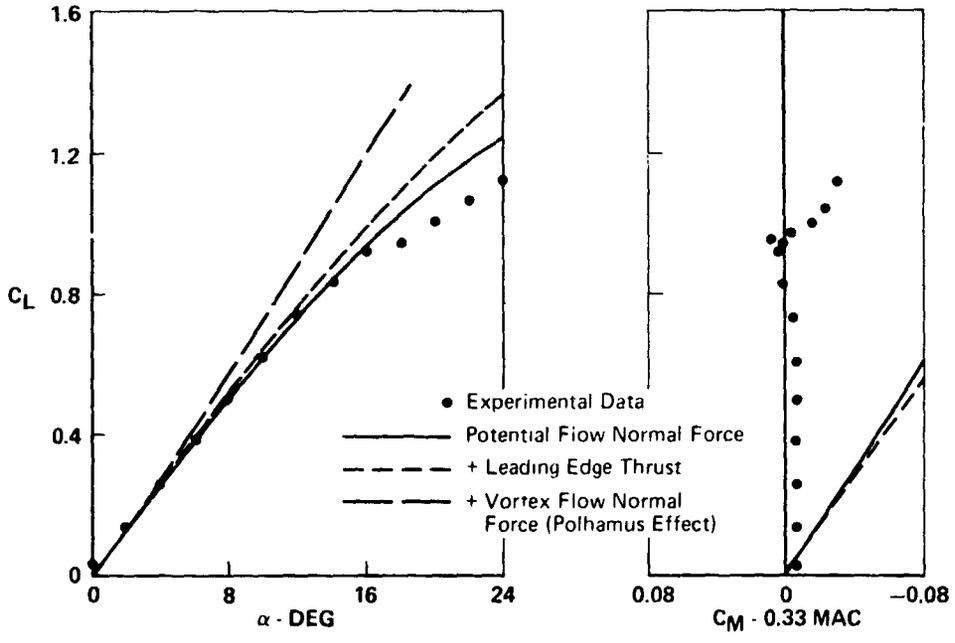

(b) Fuselage + wing + stabilator.

Figure 3.- Lift and moment polars for three configurations of the F-4E (CCV); Mach number 0.6.

C-4

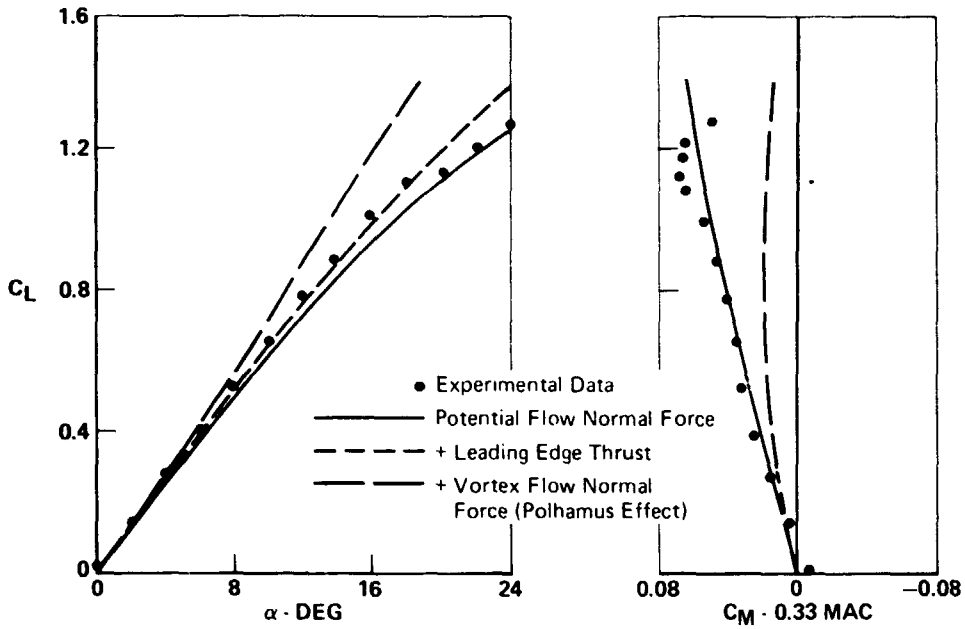

(c) Fuselage + wing + canard + stabilator.

Figure 3.- Concluded.

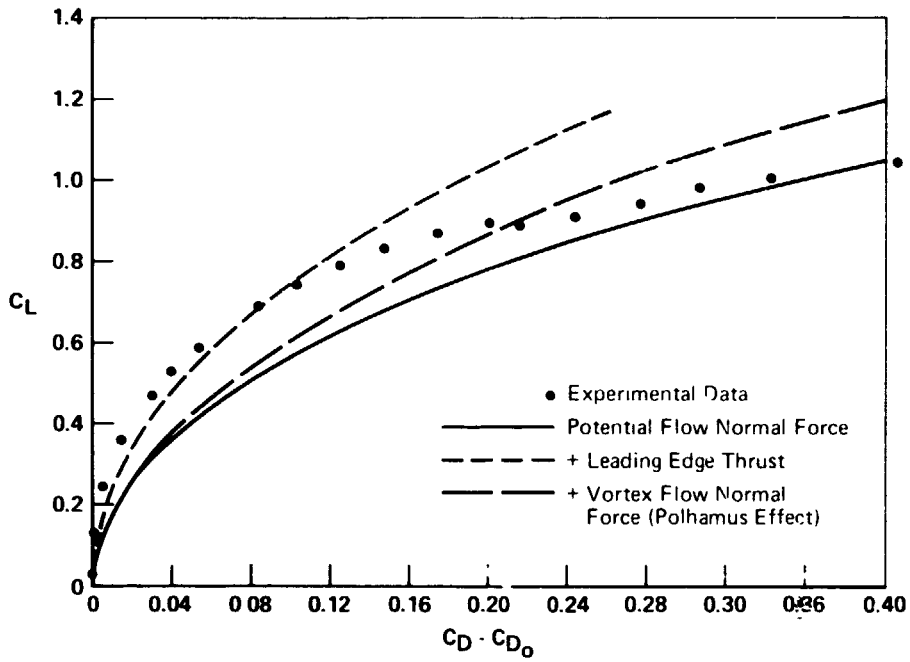

(a) Fuselage + wing.

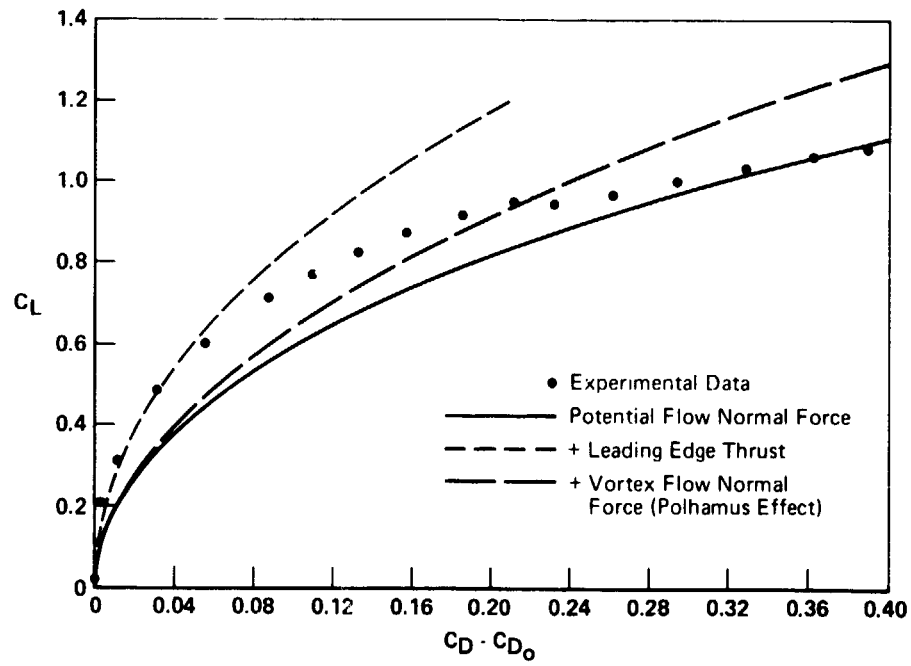

(b) Fuselage + wing + stabilator.

Figure 4.- Lift and drag polars for three configurations of the F-4E (CCV); Mach number 0.6.

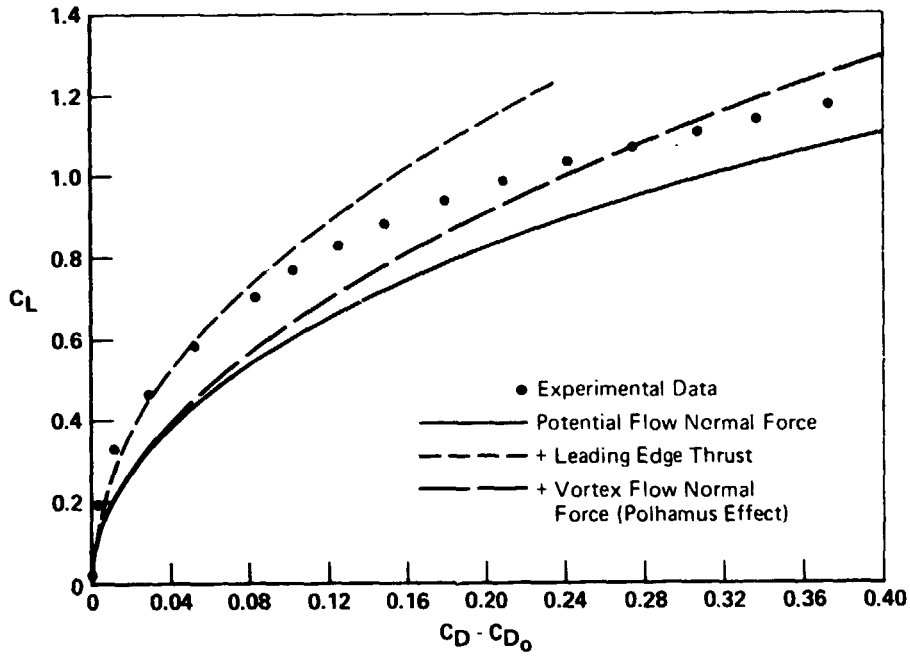

(c) Fuselage + wing + canard + stabilator.

Figure 4.- Concluded.

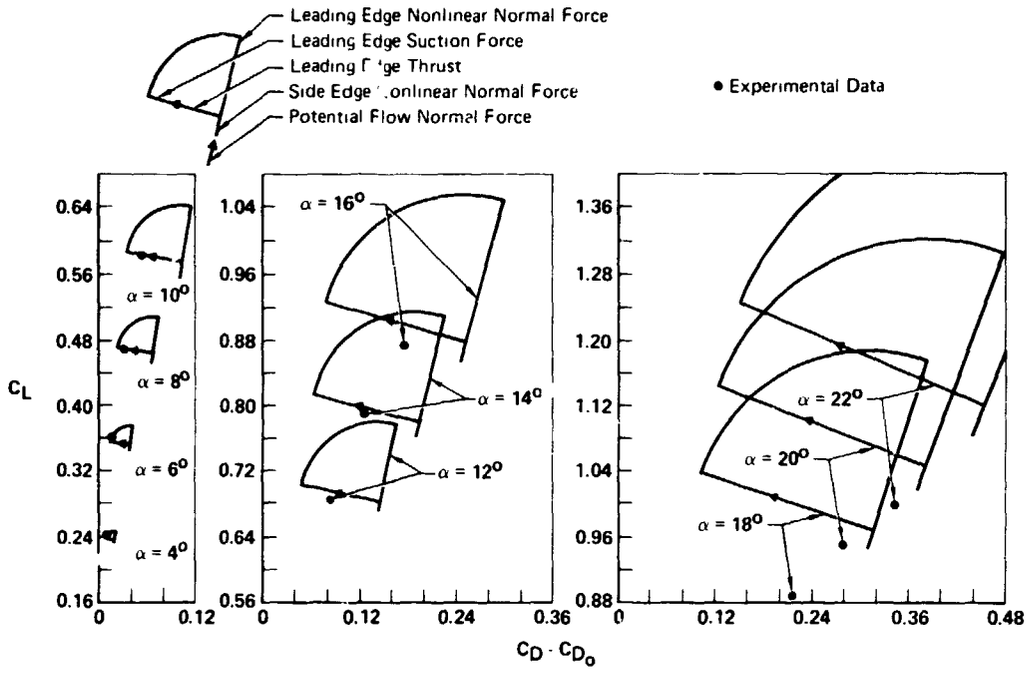

(a) Fuselage + wing.

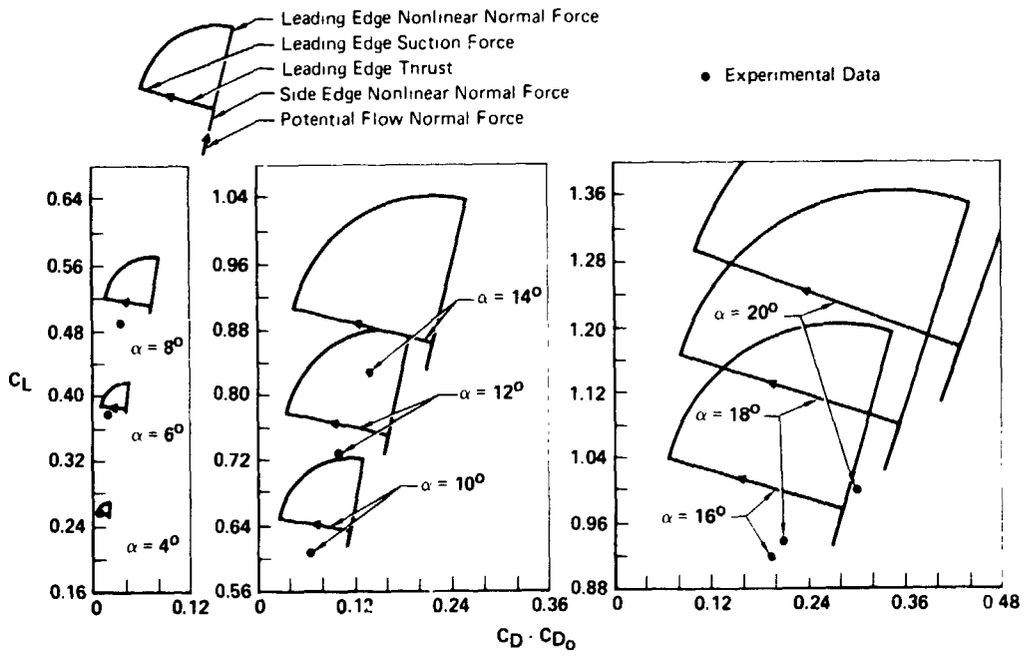

(b) Fuselage + wing + stabilator.

Figure 5.- Vectorial lift and drag polars for three configurations of the F-4E (CCV); Mach number 0.6.

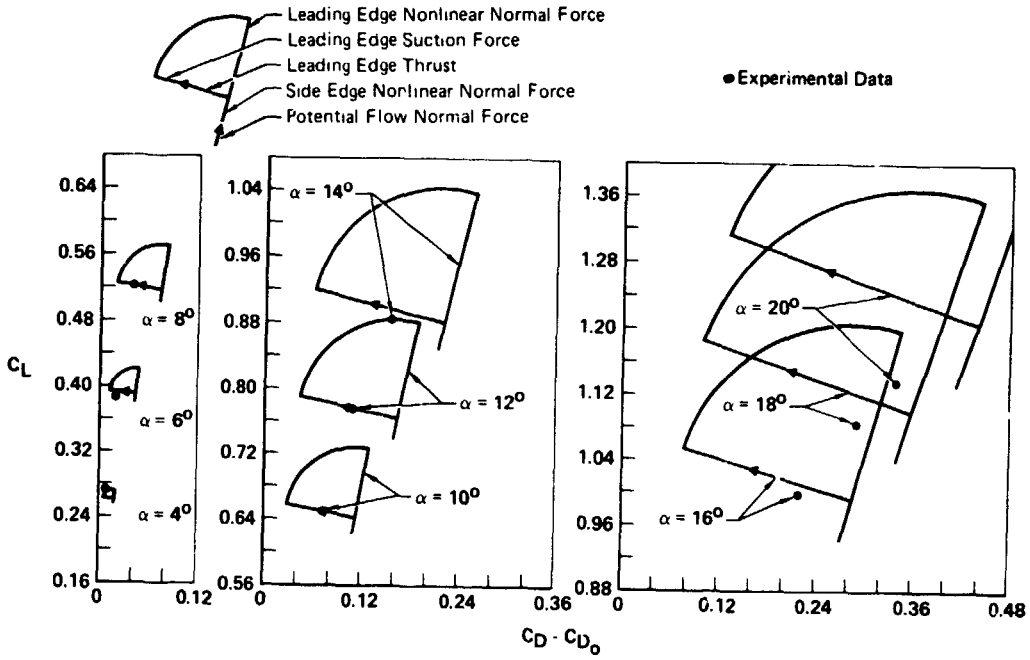

(c) Fuselage + wing + canard + stabilator.

Figure 5.- Concluded.

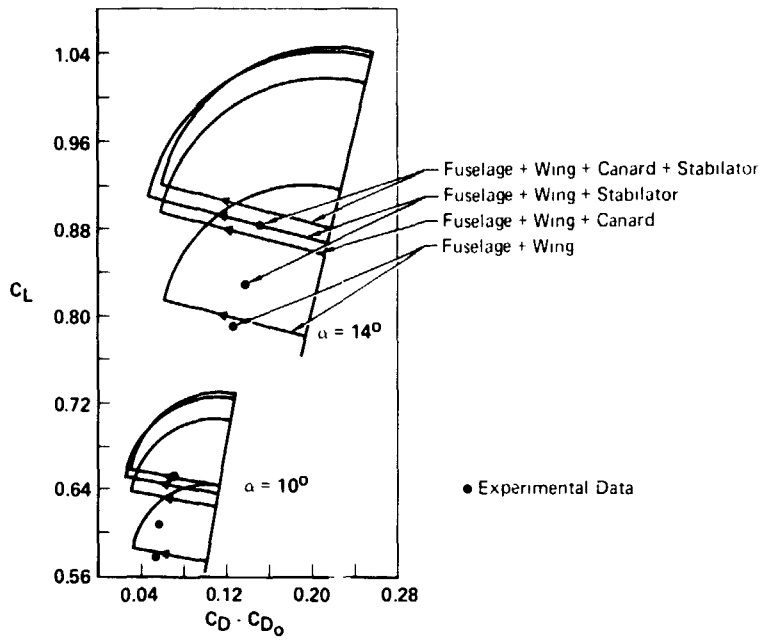

Figure 6.- Vectorial lift and drag polars at medium angles of attack for various configurations of the F-4E (CCV); Mach number 0.6.

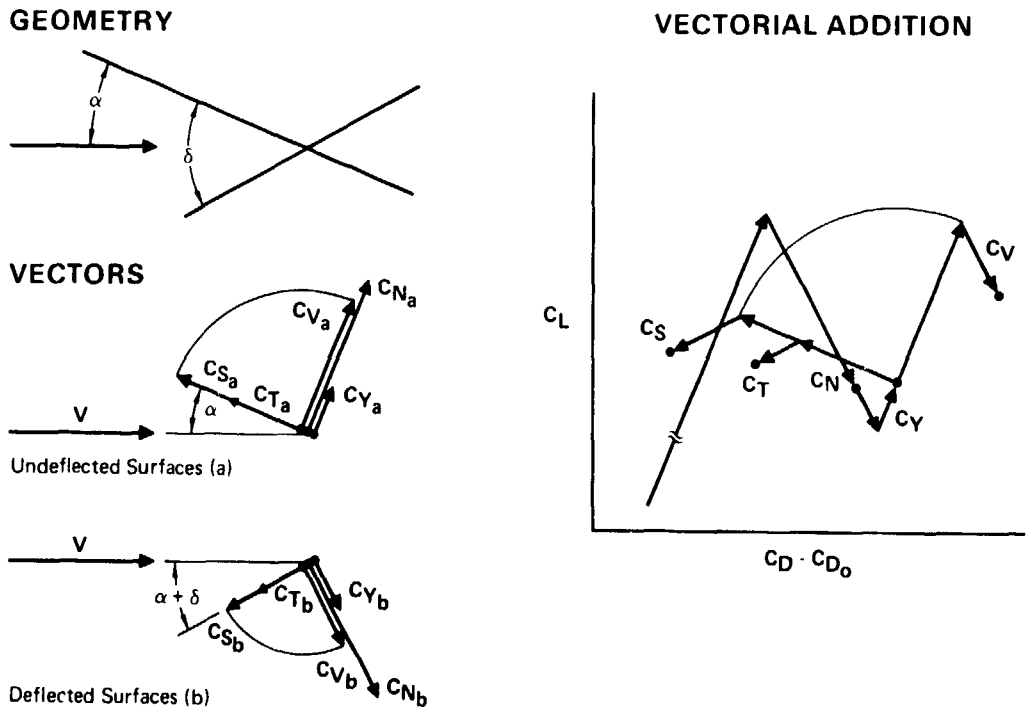

Figure 7.- Vectorial addition of lifting and control surface forces.

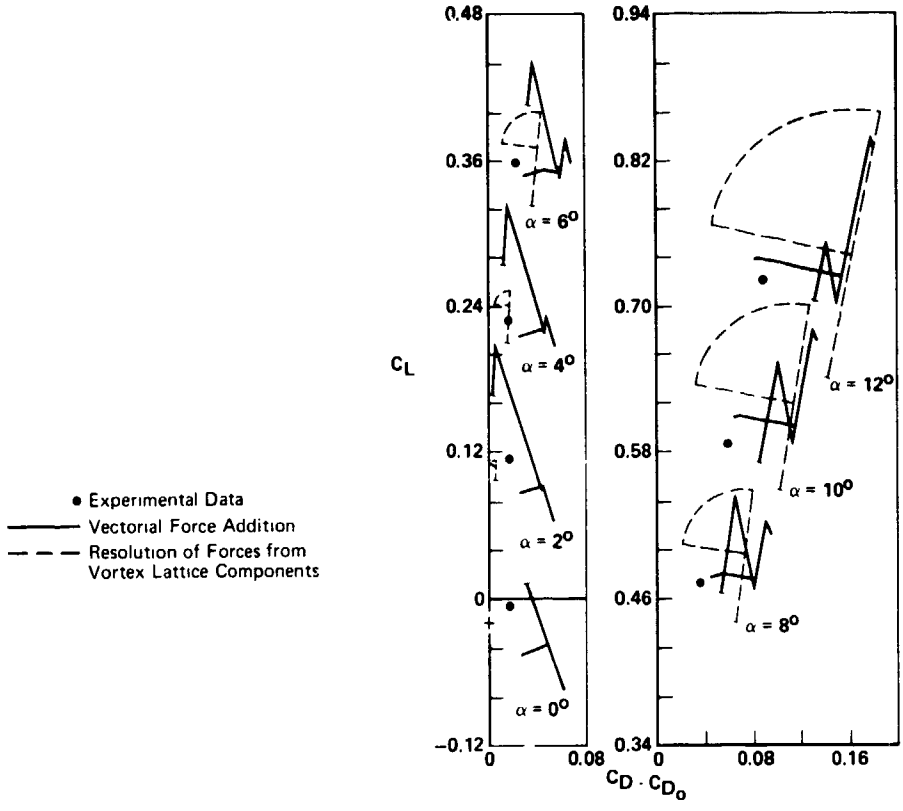

Figure 8.- Vectorial lift and drag polars for fuselage + wing + canard + stabilator; $\delta_c = -20^\circ$.

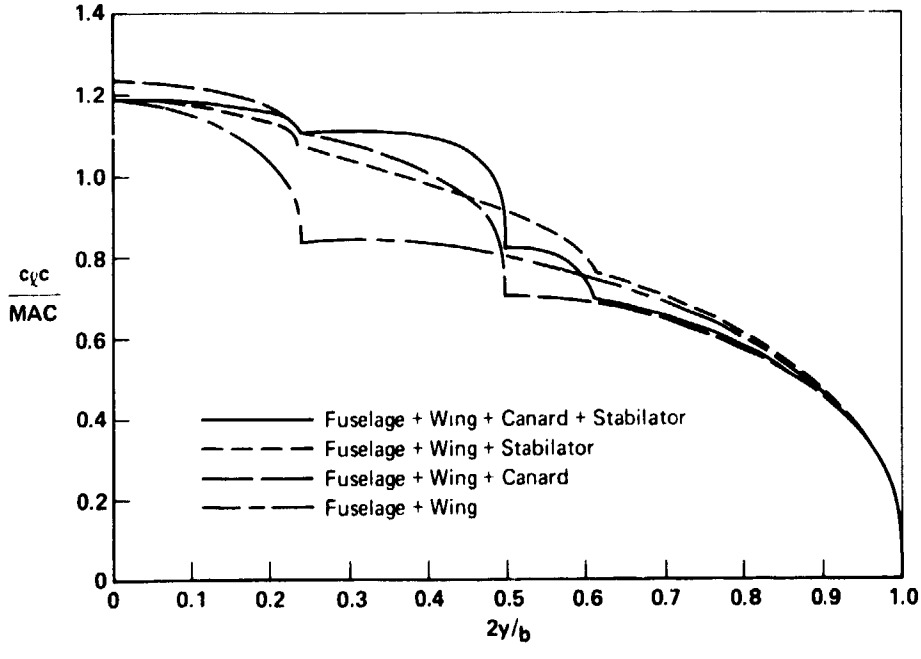

Figure 9.- Span loadings for complete configurations of the F-4E (CCV); Mach number 0.6.

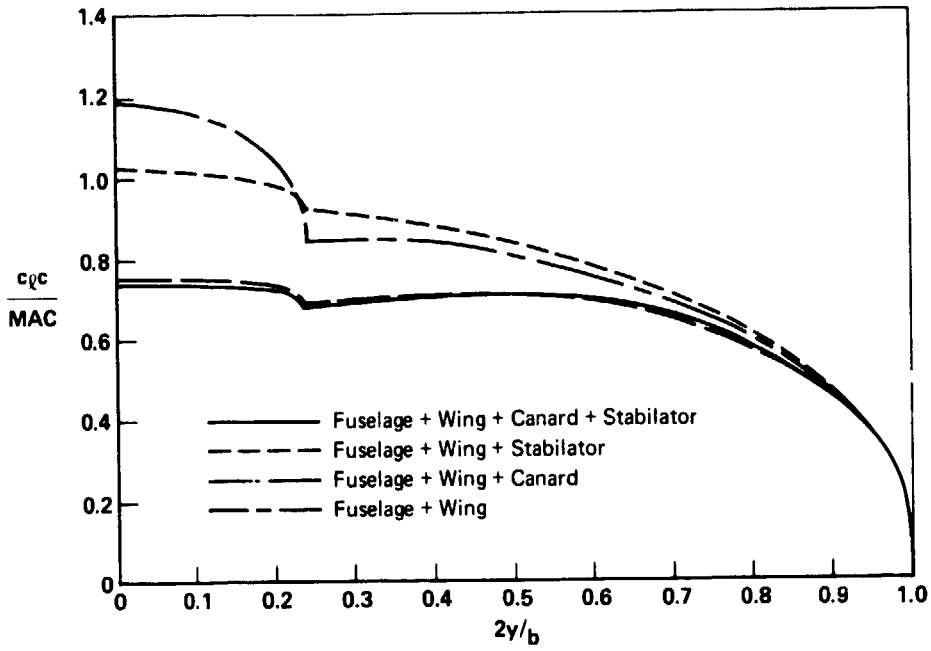

(a) Wing + partial fuselage.

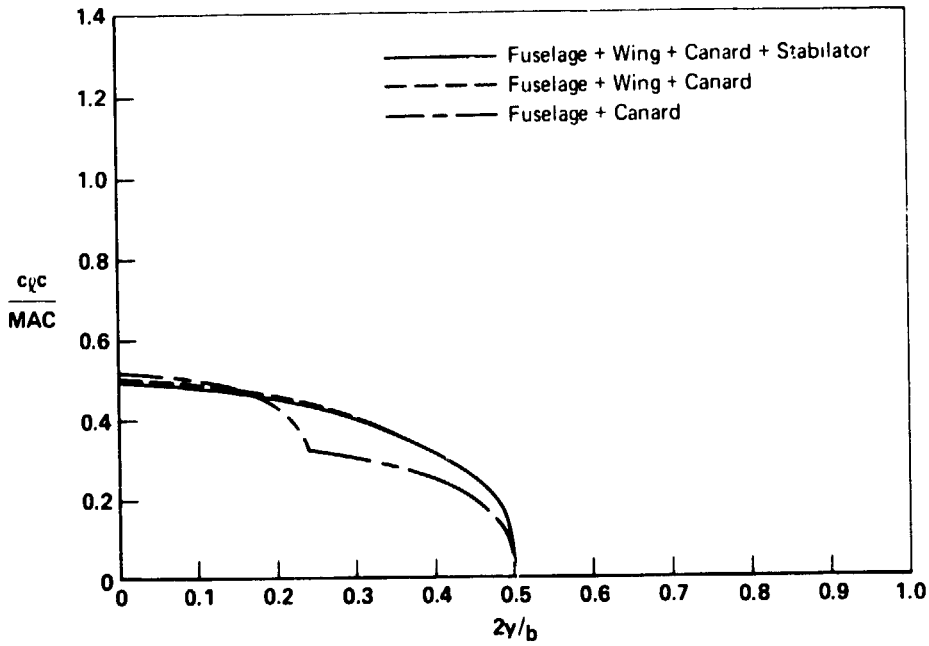

(b) Canard + partial fuselage.

Figure 10.- Span loadings for individual elements of various configurations of the F-4E (CCV); Mach number 0.6.

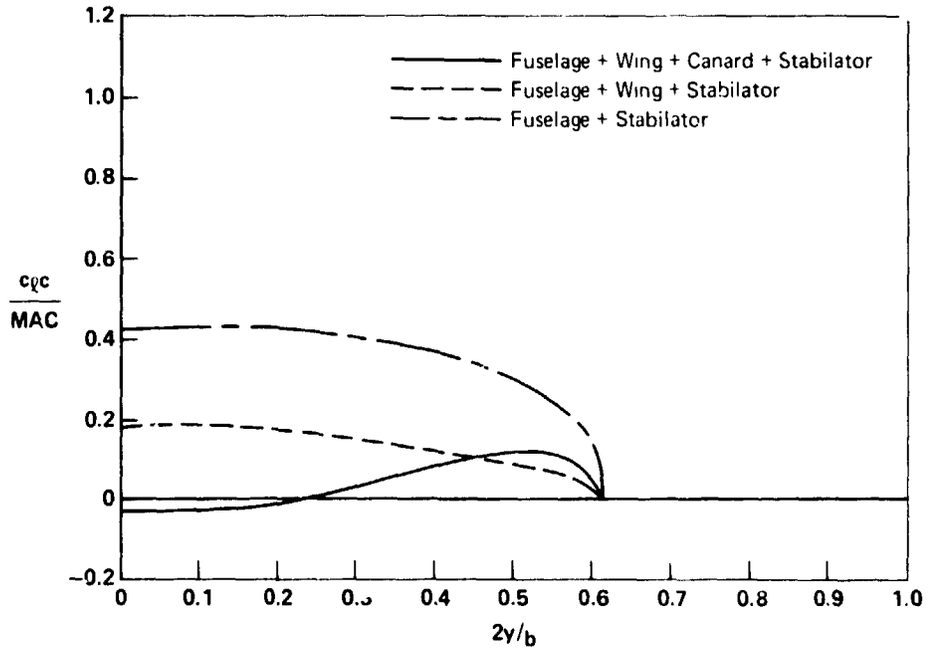

(c) Stabilator + partial fuselage.

Figure 10.- Concluded.